

Optimum Design Configuration of Dapped-End Beam Under Dynamic Loading Using TOPSIS Method

Esraa Hijah¹, Omar Najm², Hilal El-Hassan², Zubair I. Syed³

¹Al-Ain University

Abu Dhabi, United Arab Emirates

Esraa.hijah@aau.ac.ae

²United Arab Emirates University

Al Ain, United Arab Emirates

201890004@uaeu.ac.ae; helhassan@uaeu.ac.ae

³Teesside University

Middlesbrough, United Kingdom

z.syed@tees.ac.uk

Abstract – Dapped-end beams (DEBs), commonly known as half joint beams, are broadly used in bridge constructions. The reduction of the depth at the supports of the beam makes it a critical shear area and vulnerable to damage. Being used primarily on bridges, dapped-end beams are susceptible to dynamic impact loading, which is more brutal than static load cases. Various reinforcement configurations combined with different concrete properties were used to withstand the stresses generated by such loadings and mitigate their effect on the critical shear location. To reduce the extensive work and use of resources required to investigate such problems, numerical investigations were conducted on LS-DYNA software to anticipate the enhancement in the shear capacity as a function of compressive strength, main reinforcement, and shear hanger reinforcement configurations. Multi-criteria decision-making using TOPSIS analysis was conducted to choose the best scenario configuration that maximizes the beam's performance under dynamic impact loading. TOPSIS analysis was based on the deflection of the beam, shear strength of the concrete, and stress and strain of main and hanger reinforcement.

Keywords: Dapped-End Beam, Impact Loading, Critical Shear Failure, TOPSIS, Performance Index.

1. Introduction

Due to the lateral stability they provide at the support, the reduction of the overall height of the construction, and the ease of connection they provide, dapped-end beams are preferably used in pre-cast bridge constructions [1], [2]. However, the notched edge of the beam makes it vulnerable to critical shear failure due to the high-stress concentration at the half-joint to beam corner [3], [4]. Various design codes adopted special design practices to achieve adequacy against the different failure modes, such as flexural and axial tension at the extended end, direct shear at the junction, diagonal tension at the junction, diagonal tension at the extended end, and diagonal tension failure in the regular beam section [3], [4]. Design provisions such as Prestressed Concrete Institute (PCI), American Concrete Institute (ACI), and European Standards (EN) use strut-and-tie model to design the hinge location [5], which tends to have a dense and complicated reinforcement layout for conservative reasons [4]. Nevertheless, many design practices and strengthening techniques have been investigated to overcome the concentrated stress region due to the indentation in the beam. Mottok and Chan [6] suggested having the longitudinal reinforcement anchored in the nib, and sufficient hanger reinforcement will control the diagonal tension cracks propagated in the nib and entire beam section. Mitchell et al. [7] reported that concrete reinforced with closed stirrups as hanger reinforcement compared that reinforced with U-stirrups. Additionally, any reduction or elimination of part of the shear reinforcement caused premature full-depth shear failure [8]. However, reducing up to 50% of the horizontal and vertical reinforcement was possible when adding 1%, by volume, of steel fibers to the concrete mixture [9]. It was also found that adding 2%, by volume, of steel fibers without changing the reinforcing layout enhanced the ductility of the beam while increased the energy dissipation and shear capacity of the half-joint beam [2]. Nevertheless, by changing the concrete material in the nib area to Engineering Cementitious Composites (ECC), the failure load capacity was increased by 52% [10]. Meanwhile, using prestressed tendons near the re-entrant corner for strengthening reasons showed significant enhancement

in the load capacity of the dapped-end beam. Also, it was found that horizontal prestressing was more effective than vertical one [11]. A similar conclusion was derived by [4].

Despite the promising results acquired in the literature for enhancing the half-joint beam nib location, choosing the best beam configuration that enhances multi-structural responses simultaneously is not well established yet. In the past, multi-criteria decision-making (MCDM) has been applied to few civil engineering topics [12]. Most of these topics were concerning water resources and civil engineering management [12]. However, limited studies involved construction materials and structural applications [13], [14]. Simsek et al. [15] successfully optimized mixture proportions of high-strength self-compacting concrete (SCC) using the Technique for Order Preference by Similarity to Ideal Solution (TOPSIS) method. Appropriate structural systems were effectively selected in [16] using MCDM to balance materials selection and project stakeholders' judgment. Nevertheless, selecting a pile-column technology was successfully implemented using various MCDM techniques in other work [17]. MCDM in structural retrofitting applications also had its share in literature. Do and Kim [18] employed MCDM to select proper materials for concrete repair, while Sobanjo et al. [19] used MCDM for selecting the best strategy in bridge rehabilitation. Meanwhile, Billah and Alam [20] were able to select the optimum seismic retrofit technique for structural bridges. Caterino et al. [21] compared various MCDM algorithms to select the best seismic retrofitting techniques for reinforced concrete structures.

Clearly, MCDM has the potential to propose optimum scenarios for various civil engineering applications. Yet, its use in optimize the configuration of half-joint beams for superior performance. Accordingly, this work investigates the dynamic behavior of a half-joint beam against three main parameters, namely concrete compressive strength, main beam reinforcement, and hanger shear reinforcement using the LS-DYNA software analysis package. MCDM was implemented through TOPSIS method to optimize the beam configurations for maximum concrete shear stress and minimum beam deflection and stress and strain in the main and hanger reinforcements.

2. Experimental Methodology

2.1. Finite Element Modelling

Finite element (FE) modeling was conducted using LS-DYNA analysis package. All modeling techniques were developed after modeling and verification in a study conducted by Zhan et al. [22], in which the behavior of rectangular reinforced concrete beams was investigated under high impact loading. As shown in Fig. (1), the FE model of the rectangular beam showed a similar deflection result to that acquired from the experimental beam, whereby the exact modeling constraints can be used to model and analyze the dapped-end beam cases. Furthermore, an in-depth FE modeling process can be found in a previously published study by Syed et al. [23].

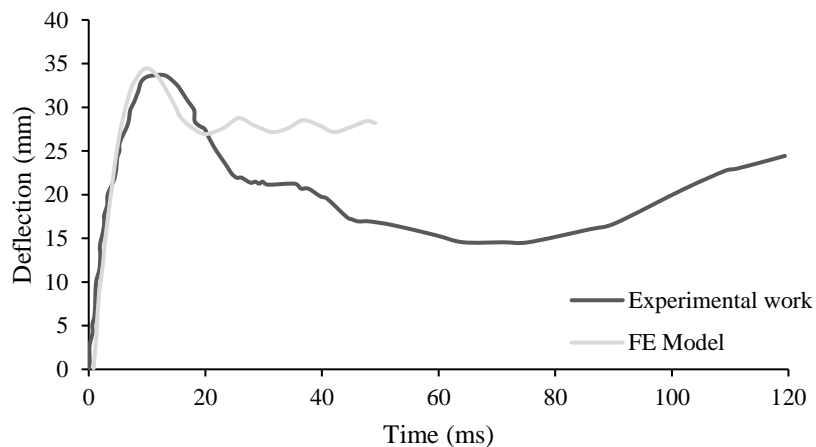


Fig. 1: Verification results of finite element modeling.

The parametric study of the dapped-end beam was conceptualized based on the experimental setup of Lu et al. [24]. Although the study was mainly concerned with static loading, the reinforcement configurations and beam geometric design were used to construct the FE control model, as illustrated in Fig. (2). The reinforcement layout is in compliance with the PCI design handbook provisions [25]. The main reinforcement of the control beam were 3#19 mm spaced at 50 mm 50 mm bars, while the hanger reinforcements used in the model were 3#13 mm with 40 mm spacing. Horizontal hoops and and flexural and shear reinforcements were provided with the minimum requirements of the PCI design handbook [25].

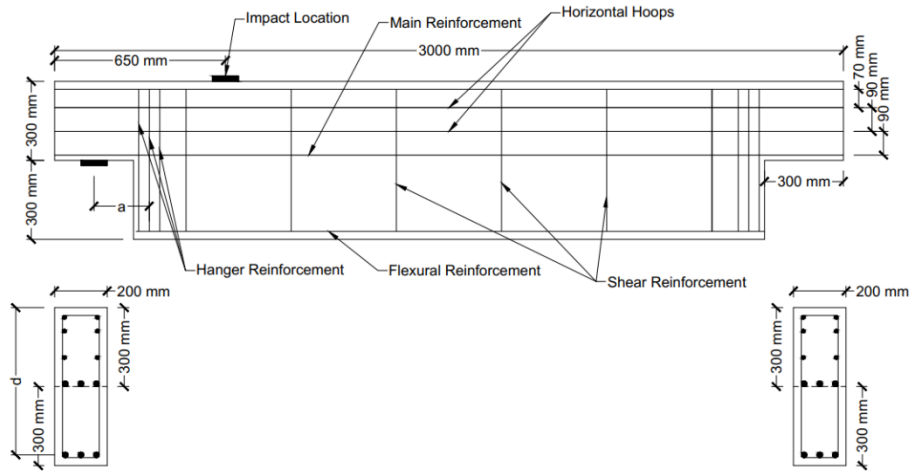


Fig. 2: Control dapped-end beam layout configurations.

The parametric study involved three main parameters, namely the hanger reinforcement layout, the main reinforcement configuration, and the concrete compressive strength. A total of 36 model cases were conducted in the following order, 7 cases concerned the hanger reinforcement configurations, designated with letter “S”, 6 cases of main reinforcement layouts, designated with letter “F”, 5 cases of compressive strength, designated with letters “Fc”, and 18 cases of combination between the flexural reinforcement and the compressive strength of concrete designated with letters “FcF”. All the cases used the same control beam configurations except for the specified designation assigned to each case. Table 1 lists the used cases in the parametric study.

Table 1: Cases included in the parametric study.

Case Designation	Specs.	Case Designation	Specs.	Case Designation	Specs.
DEB-S-1	3#10 @20 mm	DEB-F-6	2#19, 2#13 (2 layers)	DEB-FcF-3a	F3-Fc1
DEB-S-2	3#13 @20 mm	DEB-Fc-1	$f'_c = 28$ MPa	DEB-FcF-3b	F3-Fc3
DEB-S-3	5#10 @20 mm	DEB-Fc-2	$f'_c = 34$ MPa	DEB-FcF-3c	F3-Fc5
DEB-S-4	5#13 @20 mm	DEB-Fc-3	$f'_c = 40$ MPa	DEB-FcF-4a	F4-Fc1
DEB-S-5	2#13 @40 mm	DEB-Fc-4	$f'_c = 62.9$ MPa	DEB-FcF-4b	F4-Fc3
DEB-S-6	3#10 @40 mm	DEB-Fc-5	$f'_c = 75$ MPa	DEB-FcF-4c	F4-Fc5
DEB-S-7	3#16 @40 mm	DEB-FcF-1a	F1-Fc1	DEB-FcF-5a	F5-Fc1
DEB-F-1	3#22 (one layer)	DEB-FcF-1b	F1-Fc3	DEB-FcF-5b	F5-Fc3
DEB-F-2	2#19 (one layer)	DEB-FcF-1c	F1-Fc5	DEB-FcF-5c	F5-Fc5
DEB-F-3	2#25 (one layer)	DEB-FcF-2a	F2-Fc1	DEB-FcF-6a	F6-Fc1
DEB-F-4	2#19, 4#10 (2 layers)	DEB-FcF-2b	F2-Fc3	DEB-FcF-6b	F6-Fc3
DEB-F-5	3#16, 2#13 (2 layers)	DEB-FcF-2c	F2-Fc5	DEB-FcF-6c	F6-Fc5

The study aims to find the best beam configuration between the 36 model cases that provides superior performance in terms of deflection (δ), concrete shear stress (τ), and the main and hanger reinforcements stress (σ) and strain (ϵ) values. The

obtained results were taken on nodes or elements that showed the highest responses. Samples of the acquired results are listed in Table 2.

Table 2: Sample of FE results.

DEB configuration	FE Model Results					
	δ (mm)	τ (MPa)	σ_m (MPa)	ϵ_m^*	σ_h (MPa)	ϵ_h^{**}
Control	18.4	46.7	477	0.0152	354	0.00713
DEB-S-3	17.2	44.0	268	0.0152	105	0.00496
DEB-S-7	17.7	47.0	475	0.0169	378	0.00762
DEB-F-1	17.8	47.0	478	0.0151	326	0.00530
DEB-F-2	19.6	45.5	493	0.0194	391	0.01060
DEB-Fc-1	12.4	22.6	483	0.0173	373	0.00190
DEB-Fc-5	18.4	47.2	476	0.0157	387	0.00438
DEB-FcF-1c	17.3	48.2	478	0.0155	375	0.00223
DEB-FcF-2c	19.3	46.3	493	0.0195	392	0.00997

* m for main reinforcement

** h for hanger reinforcement

2.2. TOPSIS Analysis

TOPSIS was first introduced by Hwang and Yoon in 1981 [26]. Since then, it has been used as a supporting tool for decision-makers in selecting the appropriate alternative for multi-criterion problems [26]. The main principle behind its theory is defined by measuring the shortest distance of an alternative to the ideal positive solution. TOPSIS method involves six main steps to reach the final ranking criteria, obtaining the decision matrix (DM), normalizing the decision matrix, calculating the weighted normalized DM, finding the positive and negative ideal solutions, measuring the separation of each alternative from the ideal solutions, and finally calculating the relative closeness to the ideal solution.

The decision matrix comprises rows of the alternatives (DEB's configurations in this case) with columns of different attributes (the obtained results from FE-model), by which it was composed of the experimental results acquired from LS-Dyna analysis. Due to the inconsistency of units between the performances, normalization of the DM is required. The normalization of the DM can be evaluated by Eq. (1).

$$r_{ij} = \frac{a_{ij}}{\sqrt{\sum_{i=1}^m a_{ij}^2}} \quad (1)$$

Where a_{ij} represents the value of a specified performance, and r_{ij} is the normalized vector.

The weighted normalized matrix is generated after multiplying the normalized decision matrix with the corresponding assigned weight. The weights are assigned to each performance relative to their importance to the final decision result, by which the summation of the total weights should equal 1. As Dapped-end beams are critical shear members, the deflection under the impact load location, maximum shear stress of the concrete, and the stress and strain of the hanger reinforcements received the maximum weights of value 0.2. Meanwhile, the stress and strain of the main reinforcement received lower weights with a value of 0.1.

The positive and negative ideal solution (PIS, NIS) is taken through Eqs. (2) and (3), by which those equations are dependent on the performance data to be evaluated, either a benefit performance (larger is better) or cost performance (smaller is better) criteria's. When larger is the better is required for a certain performance (i.e. shear stress of concrete), the PIS is taken the maximum while the NIS is considered the minimum value of the results. In the meantime, it is the opposite when smaller is better option is of interest for certain attributes (i.e. the rest of the performances of the study).

$$A^+ = \{(\max v_{ij} | j \in J), (\min v_{ij} | j \in J')\} \quad (2)$$

$$A^- = \{(\min v_{ij} | j \in J), (\max v_{ij} | j \in J')\} \quad (3)$$

Where J is the benefit type criteria (larger is better) set and J' is the cost type criteria (smaller is better) set.

The separation measure from the ideal solution and the performance indices (PIs) are evaluated through Eqs. (4)-(6), (6), where the higher PI indicates the best DEB performance based on the weight factors assigned earlier. Table (3) list sample calculations of TOPSIS analysis, while Table (4) summarizes all the PIs for the parametric study.

$$S^+ = \sqrt{\sum_{j=1}^n (v_{ij} - v_{j^+})^2} \quad (4)$$

$$S^- = \sqrt{\sum_{j=1}^n (v_{ij} - v_{j^-})^2} \quad (5)$$

$$PI = \frac{S^-}{S^+ + S^-} \quad (6)$$

Table 3: Sample calculations of PI.

DEB config.	Normalized Weighted Decision Matrix						S _i ⁺	S _i ⁻	PI
	δ	τ	σ _m	ε _m	σ _h	ε _h			
Control	0.0358	0.0399	0.0168	0.0151	0.0324	0.0469	0.0451	0.033	0.422
DEB-S-3	0.0335	0.0376	0.0094	0.0151	0.0096	0.0326	0.0239	0.0512	0.681
DEB-S-7	0.0344	0.0402	0.0168	0.0168	0.0346	0.0501	0.0486	0.0305	0.385
DEB-F-1	0.0346	0.0402	0.0169	0.0150	0.0298	0.0348	0.0344	0.0429	0.554
DEB-F-2	0.0381	0.0389	0.0174	0.0193	0.0358	0.0697	0.0667	0.0208	0.237
DEB-Fc-1	0.0241	0.0193	0.0170	0.0172	0.0341	0.0125	0.0347	0.0598	0.632
DEB-Fc-5	0.0358	0.0404	0.0168	0.0156	0.0354	0.0288	0.0351	0.0473	0.574
DEB-FcF-1c	0.0336	0.0412	0.0169	0.0154	0.0343	0.0146	0.0289	0.0605	0.676
DEB-FcF-2c	0.0375	0.0396	0.0174	0.0194	0.0358	0.0656	0.0631	0.0219	0.257

3. Results and Discussion

As shown in Table 4, DEB-S-3 received the highest performance index value of 0.681, which indicates the highest performance between all dapped end beams in terms of deflection, shear stress, and main and hanger reinforcements stress and strain values. Indeed, the shear stress value reached 44 MPa with a minimum main reinforcement axial stress of 268 MPa and strain of 0.0152. Meanwhile, the hanger reinforcement experienced 105 MPa stress with 0.00452 maximum strain. However, the maximum deflection during the impact load reached 17.2 mm, which is considered high compared to the other cases. Nevertheless, the essence of using the TOPSIS method is to combine multiple performances and find a balance between them. The beam configurations for the highest TOPSIS ranking case were the same as the control beam except for the hanger reinforcement arrangement of which they were with less spacing and a total of 5 bars instead of 3. Conversely, DEB-F-2 showed the lowest performance indicator between all the beams with a 0.237 value (i.e., 44% lower than the control beam). The drop in the beam performance can be related to the reduction of the main reinforcement area and the spacing between them. In fact, it was depicted by analysis of variance (ANOVA) that the main steel reinforcement contributes to

about 43.4% of the performance indicators, meanwhile, 38.6% was the contribution of the concrete compressive strength. In the meantime, the hanger reinforcement received the lowest contribution to the performance indices with 18%.

From Fig. 3, all the beam configurations had PI values higher than the control mix except for DEB-F2, DEB-FcF- and DEB-S7. Although DEB-S7 has higher hanger steel area reinforcements than the control beam, its PI were slightly than the control beam. This can be related to the increase in the hanger reinforcement stress and strain values due to the crushing of the surrounding concrete elements as reinforcement size increased without increasing the concrete cover or spacing between them. As for the other two cases, the reduction of the main steel reinforcement area and the increase of spacing between the reinforcement led to mature failure of concrete which ultimately caused slight increase of about 3.4% in the stresses of the main and hanger reinforcements while caused an increase of 28% for the main reinforcement and about 49% for the hanger reinforcement. As depicted in Fig. (3-b), the increase of compressive strength beyond 40 MPa leads to a significant drop in the calculated PI except for FcF-1, where the highest main steel reinforcement area was used. It was noted from the FE results that the increase in the compressive strength induced an increase in the strain of the hanger reinforcement, which consequently reduced the PI. As the concrete strength increased from 28 MPa to 75 MPa, the strain increased in the range of 137-236% for different model cases except for FcF-1, where the drop was about 26%. The overall enhancement in the PI of the FcF-1 case was owed to the increase of the main reinforcement steel area, which indicates the importance of the main steel reinforcement configuration in the overall performance of dapped-end beams under impact loading. Nevertheless, using S3 configuration outperformed all the other cases especially in reducing the stresses in all types of reinforcements and the strain of the hanger reinforcement.

Table 4: Performance Indices (PIs) for all the cases.

Case Designation	Performance Index	Case Designation	Performance Index	Case Designation	Performance Index.
DEB-S-1	0.458	DEB-F-6	0.499	DEB-FcF-3a	0.620
DEB-S-2	0.462	DEB-Fc-1	0.632	DEB-FcF-3b	0.626
DEB-S-3	0.681	DEB-Fc-2	0.635	DEB-FcF-3c	0.423
DEB-S-4	0.604	DEB-Fc-3	0.633	DEB-FcF-4a	0.630
DEB-S-5	0.512	DEB-Fc-4	0.637	DEB-FcF-4b	0.635
DEB-S-6	0.512	DEB-Fc-5	0.574	DEB-FcF-4c	0.512
DEB-S-7	0.385	DEB-FcF-1a	0.654	DEB-FcF-5a	0.632
DEB-F-1	0.554	DEB-FcF-1b	0.654	DEB-FcF-5b	0.645
DEB-F-2	0.237	DEB-FcF-1c	0.676	DEB-FcF-5c	0.529
DEB-F-3	0.450	DEB-FcF-2a	0.516	DEB-FcF-6a	0.624
DEB-F-4	0.484	DEB-FcF-2b	0.468	DEB-FcF-6b	0.617
DEB-F-5	0.532	DEB-FcF-2c	0.257	DEB-FcF-6c	0.429

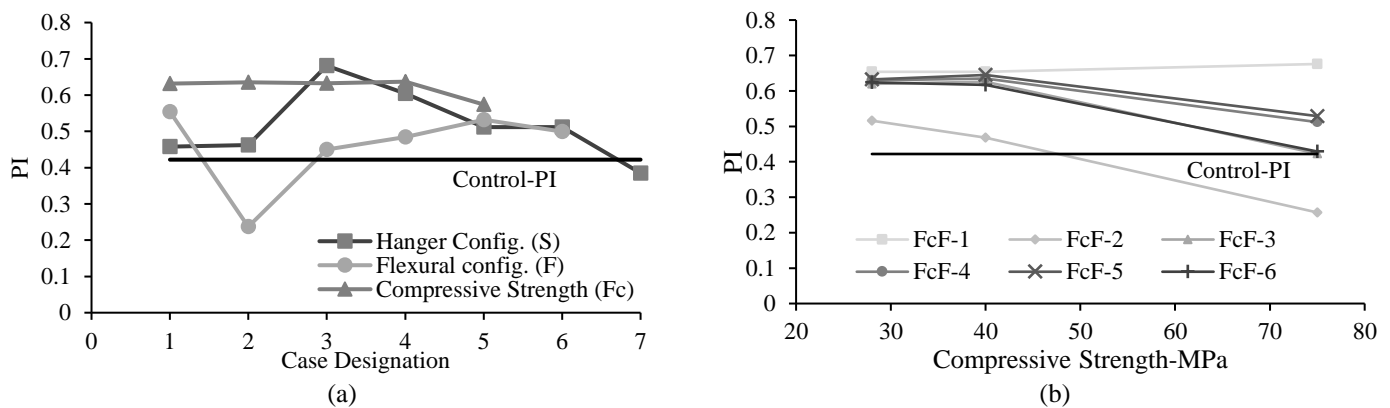


Fig. 3: (a) S, F, and Fc-DEB configurations; (b) FcF DEB configurations

4. Conclusions

TOPSIS method was successfully employed to designate the performance of various dapped end beams configurations configurations under high impact load. The parametric study involved three main parameters on the DEB performance: compressive strength, main reinforcing steel configurations, and hanger reinforcing steel configurations. The performance performance indices (PIs) were measured based on combining the effect of six major beam responses, namely, maximum deflection, concrete shear strength, main reinforcement stress and strain, and lastly, the hanger reinforcement stress and strain results. The contribution of each parameter to the PIs was measured through analysis of variance (ANOVA). The main reinforcement configurations showed a higher impact to the stability of the DEB performance under the impact load with a contribution of 43.4%; meanwhile, the contribution of the compressive strength on the performance was 38.6%. Nevertheless, the hanger reinforcement received the lowest contribution factor to the PI of 18% only. It was proven that increasing the steel reinforcing area for the main reinforcement helped reduce the strain in the hanger reinforcement that is accompanied by the increase of the concrete compressive strength. DEB-S3 received the highest PI, indicating that an increase in the number of hanger reinforcement increased the performance of half-joint beams under impact loading. Furthermore, reducing the main reinforcement caused a significant drop in the PI of the dapped-end beams. The results proved that using the TOPSIS method in structural applications can be an effective solution to MCDM problems, where different responses criteria will influence the final design considerations.

References

- [1] B. S. Mohammed, M. Aswin, and M. S. Liew, 'Prediction of failure load of RC and R-ECC dapped-end beams', *Case Studies in Construction Materials*, vol. 13, p. e00433, Dec. 2020, doi: 10.1016/j.cscm.2020.e00433.
- [2] Y. O. Özkılıç, C. Aksoylu, and M. H. Arslan, 'Experimental and numerical investigations of steel fiber reinforced concrete dapped-end purlins', *Journal of Building Engineering*, vol. 36, p. 102119, Apr. 2021, doi: 10.1016/j.jobe.2020.102119.
- [3] T. Nagy-György, G. Sas, A. C. Dăescu, J. A. O. Barros, and V. Stoian, 'Experimental and numerical assessment of the effectiveness of FRP-based strengthening configurations for dapped-end RC beams', *Engineering Structures*, vol. 44, pp. 291–303, Nov. 2012, doi: 10.1016/j.engstruct.2012.06.006.
- [4] J. Y. Moreno-Martínez and R. Meli, 'Experimental study on the structural behavior of concrete dapped-end beams', *Engineering Structures*, vol. 75, pp. 152–163, Sep. 2014, doi: 10.1016/j.engstruct.2014.05.051.
- [5] G. Sas, C. Dăescu, C. Popescu, and T. Nagy-György, 'Numerical optimization of strengthening disturbed regions of dapped-end beams using NSM and EBR CFRP', *Composites Part B: Engineering*, vol. 67, pp. 381–390, Dec. 2014, doi: 10.1016/j.compositesb.2014.07.013.
- [6] A. H. Mattock and T. C. Chan, 'Design and Behavior of Dapped-End Beams', *pcij*, vol. 24, no. 6, pp. 28–45, Nov. 1979, doi: 10.15554/pcij.11011979.28.45.
- [7] D. Mitchell, W. D. Cook, and T. Peng, 'Importance of Reinforcement Detailing', *SP*, vol. 273, pp. 1–16, Sep. 2010, doi: 10.14359/51682302.
- [8] P. Desnerck, J. M. Lees, and C. T. Morley, 'Impact of the reinforcement layout on the load capacity of reinforced concrete half-joints', *Engineering Structures*, vol. 127, pp. 227–239, Nov. 2016, doi: 10.1016/j.engstruct.2016.08.061.
- [9] N. F. Zamri, R. N. Mohamed, and K. S. Elliott, 'Shear capacity of precast half-joint beams with steel fibre reinforced self-compacting concrete', *Construction and Building Materials*, vol. 272, p. 121813, Feb. 2021, doi: 10.1016/j.conbuildmat.2020.121813.
- [10] M. Aswin, B. S. Mohammed, M. S. Liew, and Z. I. Syed, 'Shear Failure of RC Dapped-End Beams', *Advances in Materials Science and Engineering*, vol. 2015, pp. 1–11, 2015, doi: 10.1155/2015/309135.
- [11] J. Rymeš, P. Štemberk, and A. Kohoutkova, 'Experimental Analysis of Strengthening of Dapped-End Beams', *KEM*, vol. 722, pp. 241–246, Dec. 2016, doi: 10.4028/www.scientific.net/KEM.722.241.
- [12] E. K. Zavadskas, J. Antuchevičienė, and O. Kapliński, 'MULTI-CRITERIA DECISION MAKING IN CIVIL ENGINEERING: PART I – A STATE-OF-THE-ART SURVEY', *Engineering Structures and Technologies*, vol. 7, no. 3, pp. 103–113, Mar. 2016, doi: 10.3846/2029882X.2015.1143204.

- [13] O. Najm, H. El-Hassan, A. El-Dieb, 'Optimization of alkali-activated ladle slag composites mix design using taguchi-based TOPSIS method', *Constr. Build. Mater.*, vol. 327, pp. 126946, Apr. 2022, doi: <https://doi.org/10.1016/j.conbuildmat.2022.126946>.
- [14] A. El-Mir, H. El-Hassan, A. El-Dieb, and A. Alsallamin, 'Development and Optimization of Geopolymers Made with Desert Dune Sand and Blast Furnace Slag', *Sustainability*, vol. 14, no. 13, pp. 7845, doi: 10.3390/su14137845.
- [15] B. Şimşek, Y. T. İç, and E. H. Şimşek, 'A TOPSIS-based Taguchi optimization to determine optimal mixture proportions of the high strength self-compacting concrete', *Chemometrics and Intelligent Laboratory Systems*, vol. 125, pp. 18–32, Jun. 2013, doi: 10.1016/j.chemolab.2013.03.012.
- [16] P. Arroyo, I. D. Tommelein, and G. Ballard, 'Comparing AHP and CBA as Decision Methods to Resolve the Choosing Problem in Detailed Design', *J. Constr. Eng. Manage.*, vol. 141, no. 1, p. 04014063, Jan. 2015, doi: 10.1061/(ASCE)CO.1943-7862.0000915.
- [17] E. K. Zavadskas, S. Sušinskas, A. Daniūnas, Z. Turskis, and H. Sivilevičius, 'Multiple criteria selection of pile-column construction technology', *Journal of Civil Engineering and Management*, vol. 18, no. 6, Art. no. 6, Nov. 2012, doi: 10.3846/13923730.2012.744537.
- [18] J.-Y. Do and D.-K. Kim, 'AHP-Based Evaluation Model for Optimal Selection Process of Patching Materials for Concrete Repair: Focused on Quantitative Requirements', *Int J Concr Struct Mater*, vol. 6, no. 2, pp. 87–100, Jun. 2012, doi: 10.1007/s40069-012-0009-9.
- [19] J. O. Sobanjo, G. Stukhart, and R. W. James, 'Evaluation of Projects for Rehabilitation of Highway Bridges', *Journal of Structural Engineering*, vol. 120, no. 1, pp. 81–99, Jan. 1994, doi: 10.1061/(ASCE)0733-9445(1994)120:1(81).
- [20] A. H. M. M. Billah and M. S. Alam, 'Performance-based prioritisation for seismic retrofitting of reinforced concrete bridge bent', *Structure and Infrastructure Engineering*, vol. 10, no. 8, pp. 929–949, Aug. 2014, doi: 10.1080/15732479.2013.772641.
- [21] N. Caterino, I. Iervolino, G. Manfredi, and E. Cosenza, 'Comparative Analysis of Multi-Criteria Decision-Making Methods for Seismic Structural Retrofitting', *Computer-Aided Civil and Infrastructure Engineering*, vol. 24, no. 6, pp. 432–445, 2009, doi: 10.1111/j.1467-8667.2009.00599.x.
- [22] T. Zhan, Z. Wang, and J. Ning, 'Failure behaviors of reinforced concrete beams subjected to high impact loading', *Engineering Failure Analysis*, vol. 56, pp. 233–243, Oct. 2015, doi: 10.1016/j.engfailanal.2015.02.006.
- [23] Z. I. Syed, E. S. Hejah, and O. A. Mohamed, 'Modelling of Dapped-End Beams under Dynamic Loading', *IJMERR*, pp. 242–247, 2017, doi: 10.18178/ijmerr.6.3.242-247.
- [24] W. Lu, I. Lin, S. Hwang, and Y. Lin, 'Shear strength of high-strength concrete dapped-end beams', *Journal of the Chinese Institute of Engineers*, vol. 26, no. 5, pp. 671–680, Jul. 2003, doi: 10.1080/02533839.2003.9670820.
- [25] Precast/Prestressed Concrete Institute, *PCI Design Handbook, 8th Edition*. Precast/Prestressed Concrete Institute, 2017. doi: 10.15554/MNL-120-17.
- [26] Y. Çelikkbilek and F. Tüysüz, 'An in-depth review of theory of the TOPSIS method: An experimental analysis', *Journal of Management Analytics*, vol. 7, no. 2, pp. 281–300, Apr. 2020, doi: 10.1080/23270012.2020.1748528.